THICKNESS OF LIQUID FILM FORMED IN SLUG FLOW IN MICRO TUBE

Youngbae Han and Naoki Shikazono

Department of Mechanical Engineering, The University of Tokyo
Hongo 7-3-1, Bunkyo-ku, Tokyo, 113-8656, Japan

ABSTRACT

Slug flow is the representative flow regime of two-phase flow in micro tubes. It is well known that the evaporation of thin liquid film formed between the tube wall and the vapor bubble plays a important role in micro conduits heat transfer. In the present study, experiments are carried out to clarify the effect of parameters that affect the formation of the thin liquid film. Laser focus displacement meter is used to measure the thickness of the thin liquid film. Air, ethanol, water and FC-40 are used as working fluids. Circular tubes with five different diameters, D = 0.3, 0.5, 0.7, 1.0 and 1.3 mm, are used. It is confirmed that the liquid film thickness is determined only by capillary number at small capillary number and the effect of inertia force on the liquid film thickness is negligible. But as capillary number increases, the effect of inertia force is not neglected. At relatively high capillary number, liquid film thickness shows minimum against Reynolds number. The effects of bubble length, liquid slug length and gravity on liquid film thickness are investigated. Experimental correlation based on the capillary number, Reynolds number and Weber number is proposed.

INTRODUCTION

Micro scale evaporation heat transfer attracts much attention due to its many advantages, e.g., high efficiency, miniaturization, etc. However, the characteristics of flow boiling in micro tube is quite different from those in conventional tube and they are not fully understood. Flow regime is also different in micro tube due to surface tension, and slug flow becomes the dominant flow pattern. It is known that the evaporation of thin liquid film formed between the tube wall and the vapor bubble plays a important role in micro tube heat transfer. It is reported that the thickness of the liquid film is one of the important factors for the prediction of flow boiling heat transfer in micro tubes [1][2]. Many researches on the liquid film formed in slug flow in micro tube have been conducted both experimentally and theoretically.

Taylor [3] experimentally obtained the mean liquid film thickness remaining on the wall by measuring the difference of the bubble velocity and the fluid mean velocity. He used highly viscous fluid, e.g., glycerine, syrup-water mixture and lubricating oil, so wide range of capillary number was covered in his experimental data.

Bretherton [4] suggested a scaling analysis of the liquid film thickness with the lubrication approximation. He showed that the liquid film thickness can be scaled with $Ca^{2/3}$.

Moriyama et al. [5] obtained the liquid film thickness formed by a vapor bubble expansion in a narrow gap by measuring the temperature change of the channel wall, which was superheated initially. In his experiment, the heat is assumed to be consumed by the evaporation of the liquid film. His experimental data was correlated in terms of capillary number and Bond number based on the interface acceleration.

Heil [7] investigated the effect of inertia force on the liquid film thickness numerically. It is shown that the liquid film thickness and the pressure gradient are dependent on the Reynolds number.

Aussillous and Quere [6] measured the liquid film thickness using fluids of relatively low surface tension. It was found that the liquid film thickness deviates from the Taylor's data at relatively high capillary number. Visco-inertia regime, where the effect of inertia force on the liquid film thickness becomes significant was demonstrated.

Kreutzer et al. [8] investigated the liquid film thickness and the pressure drop in a micro tube both numerically and experimentally. Their predicted liquid film thickness showed almost the same trend with that of Heil [7].

Utaka et al. [9] measured the liquid film thickness formed by a vapor bubble in a narrow gap mini-channel with laser extinction method. They investigated heat transfer characteristics quantitatively. It was concluded that the boiling phenomena were determined by two kinds of characteristic periods, i.e., the micro-layer dominant and the liquid saturated periods.

Although many experiments have been carried out to measure the liquid film thickness in micro tubes, quantitative data of the liquid film thickness and the varying liquid film thickness are still limited. To develop a good flow boiling heat transfer model in micro tube, it is crucial to know the characteristics of the local liquid film thickness. In the present study, the local liquid film thickness and varying liquid film thickness are measured directly with laser focus displacement meter. Series of experiments is conducted to investigate the effects of important parameters that affect the formation of liquid film in micro tubes.

EXPERIMENTAL SETUP AND PROCEDURE

Experimental Setup

Circular tubes made of Pyrex glass with 0.3, 0.5, 0.7, 1.0 and 1.3 mm inner diameter were used as test tubes. Tube diameter was measured by microscope and the inlet and outlet inner diameters were averaged. Table 1 and Fig. 1 show the dimensions

Table 1. Dimensions of test tubes

Tube	I.D. (mm)	O.D. (mm)	Length (mm)
A	1.305	1.6	250
B	0.995	1.6	250
C	0.715	1.0	250
D	0.487	0.8	250
E	0.305	0.5	250

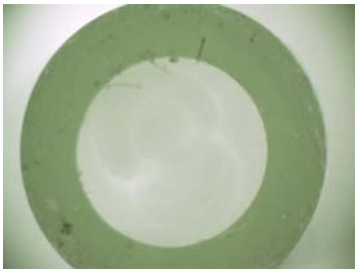

Figure 1. Photograph of 0.995 mm inner diameter tube

Table 2. Properties of the working fluids at 25°C and 1 atm

	Water	Ethanol	FC-40
ρ (kg/m^3)	997	785	1849
μ (μ Pa · s)	889	1088	3260
σ (mN/m)	70.0	22.3	16.0

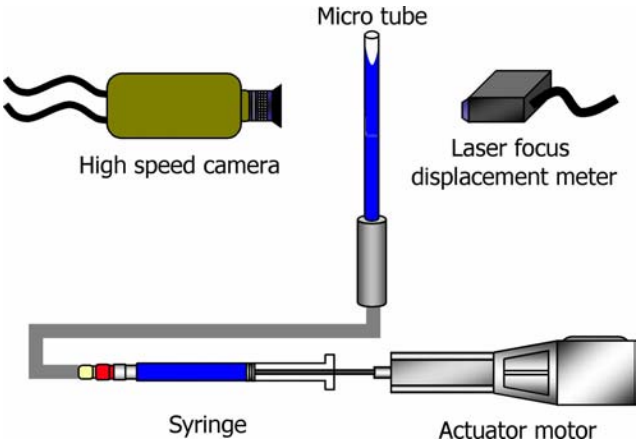

Figure 2. Schematic diagram of the experimental setup

and the photograph of the test tubes. The difference of inlet and outlet inner diameters is less than 1% for all tubes. Ethanol, water, FC-40 (Fluorinert, 3M) and air were used as working fluids. All experiments were conducted under conditions of room temperature and 1 atm. Table 2 shows the properties of each fluid at 25°C and 1 atm.

Figures 2 and 3 show the schematic diagram and the photograph of the experimental setup. One edge of Pyrex glass tube was connected to the syringe and the actuator motor. Actuator motor (EZHC6A-101, Oriental motor) was used to move the liquid inside the test conduits. The velocity range of actuator motor is 0 to 0.6 m/s. Syringes with several cross sectional areas were used to control the liquid velocity in micro tube. The range of liquid velocity in present experiments was 0 to 6 m/s.

The velocity of the gas-liquid interface was measured from the images captured by the high speed camera (Phantom 7.1). The images were taken at several frame rates according to the bubble velocity. For maximum bubble velocity, frame rate was 10000 frames per second with a shutter time of 10 μs.

Laser focus displacement meter (LT9010M, Keyence) was used to measure the thickness of the liquid film. Figure 4 shows the principle of the laser focus displacement meter. The displacement of target surface can be determined by the displacement of objective lens moved by the tuning fork. The received light intensity becomes highest in the light-receiving element when focus is obtained on the target surface. The resolution is 0.01 μm, the laser spot diameter is 2 μm and the response time is 640 μs. Thus, it is possible to measure the varying local thickness of liquid film. Laser focus displacement meter has been used by several researchers for the measurement of liquid film thickness [10][11]. It is reported that the laser focus displacement meter can measure the liquid film thickness very accurately, within 1% error [11]. Liquid film thickness is transformed to DC voltage signal in the range of $\pm$10V. Output signal was sent to PC through GPIB interface and recorded with LabVIEW.

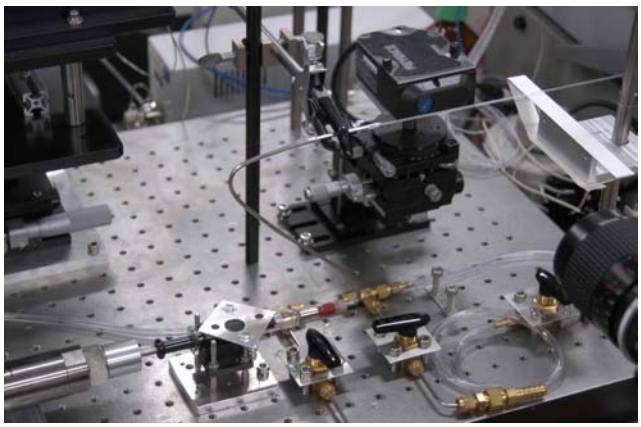

Figure 3. Photograph of experimental setup

Experimental Procedure

The experimental procedure is described in this section. Cover glass and glycerol were used to remove the focus scattering caused by the curvature of the outer wall. Refractive index of glycerol (n = 1.47) is almost the same with that of the Pyrex glass (n = 1.474), so the refraction of laser between glycerol and Pyrex glass can be neglected. Figure 5 shows the schematic diagram of the micro tube with cover glass and glycerol.

It is difficult to detect the interface of the inner wall and the liquid film at the same time, because the difference of both two refractive indexes is small. Therefore, the distance from the cover glass to the inner wall is initially measured without liquid film. Then, the thickness including liquid film is measured. The liquid film thickness is calculated from the difference of these two values.

Although the focus scattering caused by the curvature of the outer wall is removed, there is another focus scattering due to the curvature of the inner wall. To compensate for this

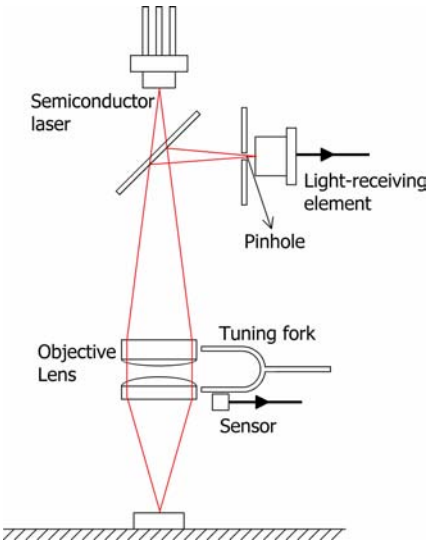

Figure 4. Principle of laser focus displacement meter

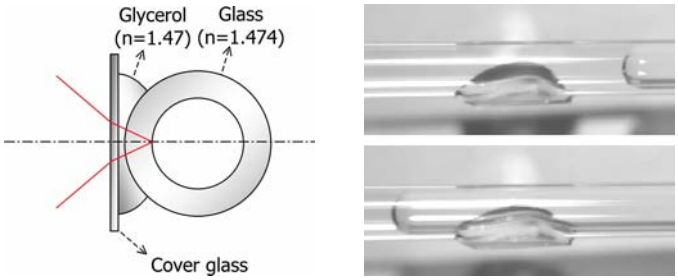

Figure 5. Schematic of micro tube and images of bubble movement

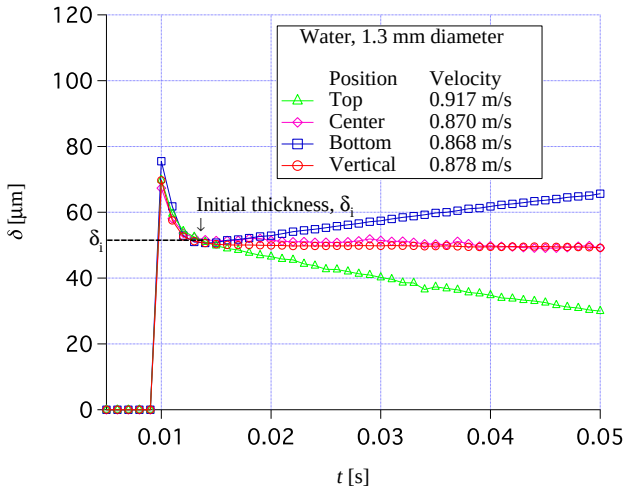

Figure 6. Measured liquid film thickness against time

inner wall scattering, correction suggested by Takamasa and Kobayashi [10] was used. Focus scattering due to inner wall is less than 1% of liquid film thickness.

Figure 6 shows an typical measurement example. Inner diameter of the tube is 1.3 mm and working fluid is water. The liquid film thicknesses were measured at four different positions, top, center and bottom in horizontal flow direction and vertical flow direction. There is no signal before the air-liquid interface passes by the measuring position because micro tube is filled with liquid. After air-liquid interface passes by the measuring position, liquid film is formed on the wall and signal is obtained

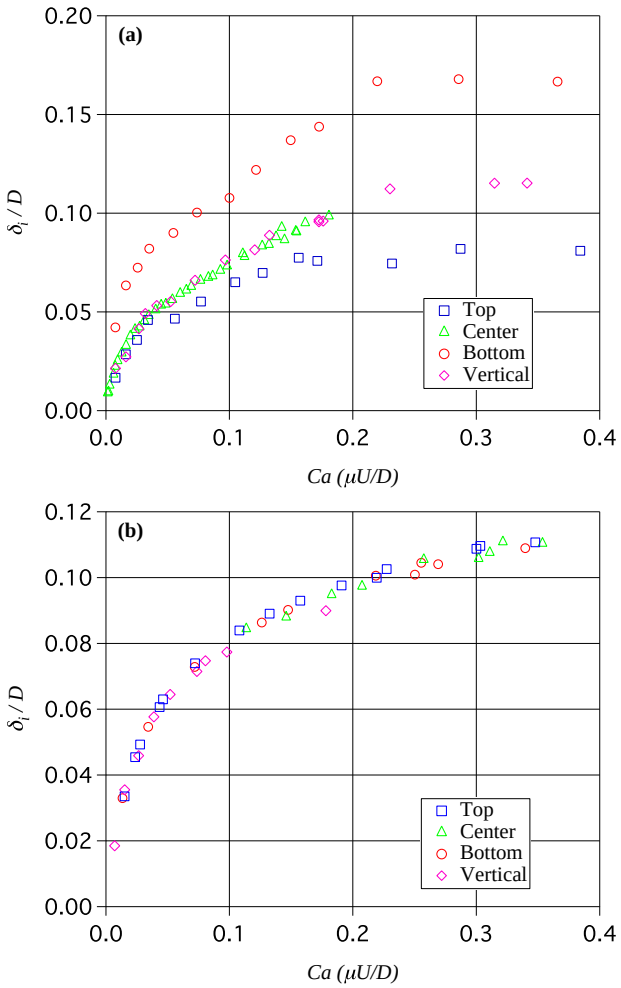

Figure 7. Initial liquid film thickness,δ_i measured at different positions: (a) FC-40, 1.3 mm diameter tube (b) FC-40, 0.3 mm diameter tube

by the laser focus displacement meter. The laser focus displacement meter can detect the interface where the angle is less than 11°.

In Fig. 6, liquid film thicknesses decrease initially and then become constant or change lineally. Initial decrease part is the transition region between bubble nose and the flat film region. The reason for the lineal change after the initial drop is considered to be the effect of gravity. The liquid film flows down slowly due to gravity after liquid film is formed on the tube wall. On the contrary, liquid film thicknesses at center in horizontal flow and vertical flow do not change but remain almost constant. Regardless of the measuring position, initial liquid film thicknesses δ_i are almost the same. This initial liquid film thickness δ_i is collected as experimental data. When the effect of gravity becomes dominant, initial liquid film thickness becomes different according to the measuring position.

The Effect of Gravity on Initial Thickness

Figure 7 shows the initial thicknesses measured at each position in 1.3 mm and 0.3 mm inner diameter tubes, respectively. In 1.3 mm inner diameter tube, initial thicknesses are different depending to the measuring position. Initial thicknesses at center in horizontal flow direction and vertical flow direction are almost the same. On the contrary, initial thicknesses in 0.3 mm inner diameter tube are almost the same regardless of the mea-

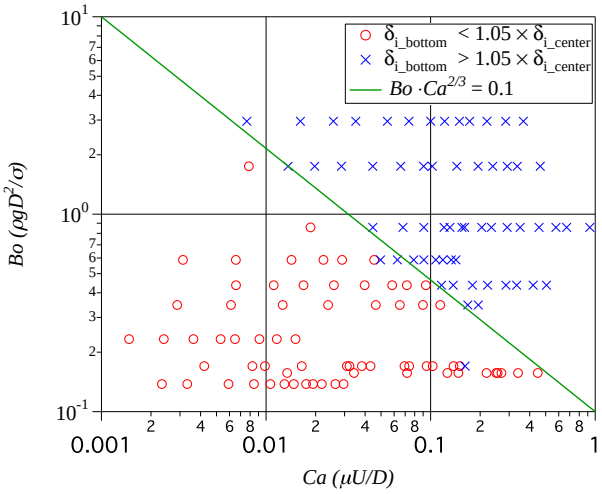

Figure 8. Criterion for the effect of gravity on the initial thickness

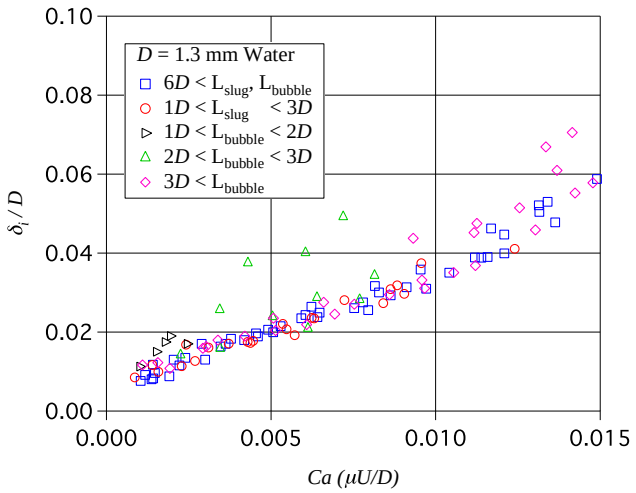

Figure 9. The effects of bubble length and liquid slug length on liquid film thickness

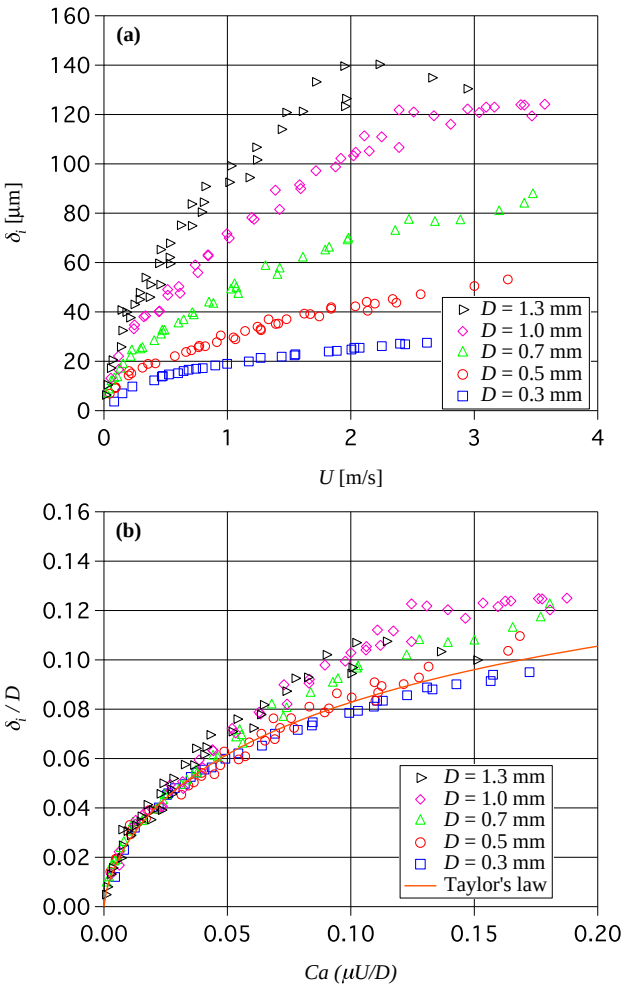

Figure 10. The results using ethanol: (a) Liquid film thickness against bubble velocity (b) Dimensionless liquid film thickness (δ_i/D) against capillary number ($Ca = \mu U/\sigma$)

suring position.

Figure 8 shows the criterion for the effect of gravity on initial thickness. In Fig. 8, cross marks correspond to the cases when initial thickness at the bottom are more than 5% larger than that at the center, and circle marks are for the opposite cases. In Fig. 8, the solid line shows $Bo{\cdot}Ca^{2/3} = 0.1$ and this is used as the criterion for the effect of gravity on the initial liquid film thickness.

The Effects of Bubble Length and Liquid Slug Length

In the present experiment, air-liquid interface is pulled by the actuator motor. Thus, the flow can be considered as a very long bubble after a very long liquid slug. In reality, bubble length and liquid slug length could be shorter and it is considered that they may affect the liquid film thickness. The effects of bubble length and liquid slug length were investigated. Water is used as working fluid and liquid film thickness is measured at the tube bottom in horizontal flow direction. Air bubble and liquid slug are injected at the open edge of the test tube. Bubble and liquid slug lengths are measured from the images captured by high speed camera. Bubble length L_{bubble} and liquid slug length L_{slug} are varied within the range of $D < L_{bubble}, L_{slug} < 6D$.

Figure 9 shows measured δ_i with different L_{bubble} and L_{slug}. It seems that there is no effect of L_{slug} on the liquid film thickness. On the other hand, bubble length seems to affect the liquid film thickness, i.e., liquid film formed after shorter bubbles seems to be thicker. If the bubble length becomes 3 times larger than the inner diameter, liquid film thickness becomes almost the same as the case of a long bubble and a long liquid slug. Liquid film becomes thicker near the bubble tail. It is thought that the liquid film thickness of short bubbles becomes thicker because the bubble tail affects δ_i. Transition region length between bubble nose and flat film region is proportional to capillary number in Bretherton's theory [4]. Thus, At high capillary number, we can observe some deviations for $L_{bubble} > 3D$ in Fig. 9.

RESULT AND DISCUSSION

Experimental Results using Ethanol

Figure 10 (a) shows the liquid film thickness against bubble velocity for ethanol. Liquid film thicknesses measured at the tube center in horizontal flow are used. Liquid film thickness increases with bubble velocity and tube diameter. It is known that the liquid film thickness is mainly determined by the force bal-

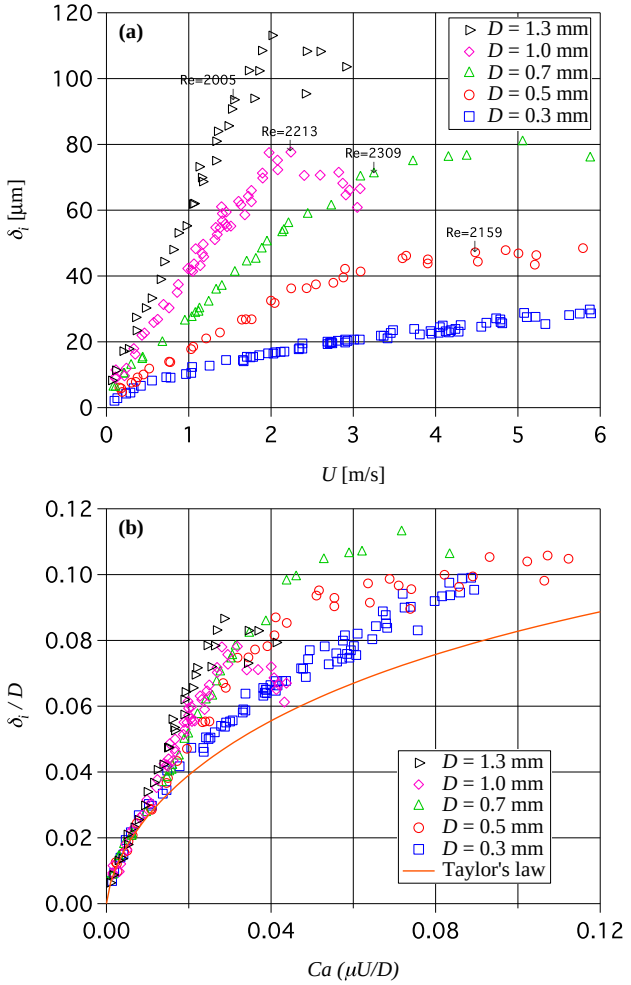

Figure 11. The results using water: (a) Liquid film thickness against bubble velocity (b) Dimensionless liquid film thickness (δ_i/D) against capillary number ($Ca = \mu U/\sigma$)

ance between the viscous force and surface tension, which can be represented by capillary number, $Ca = \mu U/\sigma$. It is considered that the effect of viscous force dominates as bubble velocity and tube diameter increase.

Figure 10 (b) shows the dimensionless liquid film thickness, δ_i/D against capillary number, using the same data. The solid line in Fig. 10 (b) is an empirical curve fitting of Taylor's experimental data proposed by Aussillous and Quere [6].

$$\frac{\delta}{R} = \frac{1.34Ca^{\frac{2}{3}}}{1+2.5\times1.34Ca^{\frac{2}{3}}}. \quad (1)$$

Equation (1) is called Taylor's law. At low capillary number, dimensionless liquid film thicknesses of five tubes become nearly identical. However, as capillary number increases, the liquid film thicknesses in larger diameter tubes show slightly larger values. This can be attributed to the effect of inertia force. The inertia force is usually neglected in micro scale, but there is still some inertia effect left at high capillary numbers.

Experimental Results using Water

Then, Water is used as a working fluid. The Reynolds number of water is about 6 times larger than that of ethanol at the same capillary number. Figures 11 (a) and (b) show the liquid

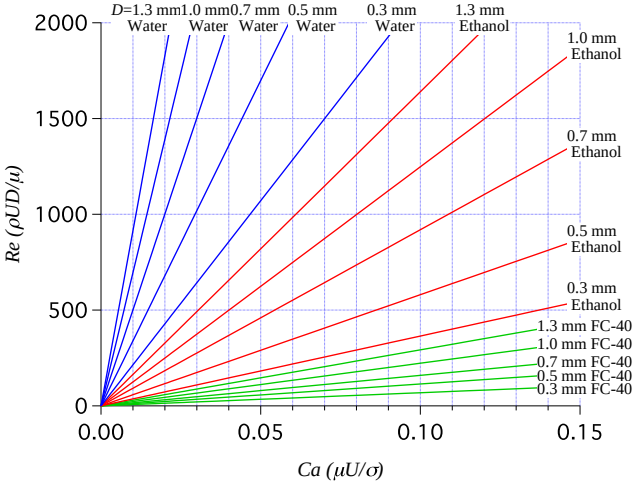

Figure 12. Reynolds number against capillary number

film thickness and the dimensionless liquid film thickness, δ_i/D. The solid line in Fig. 11 (b) is the Taylor's law, i.e., Eq. (1). The working fluids in Taylor's experiments were highly viscous such as glycerol and sugar-water syrup. Therefore, Reynolds number in his experiment was quite small and the inertia force was negligible. The dimensionless liquid film thickness of water shows much larger value than that of ethanol and the Taylor's law. It is considered that the effect of inertia force on liquid film thickness becomes large and inertia force make liquid film thickness thicker as capillary number increases.

As shown in Fig. 11 (a), the trend of liquid film thickness is changed when the Reynolds number becomes larger than roughly 2000. Reynolds number is defined as $Re = \rho UD/\mu$. For $Re > 2000$, liquid film thickness against capillary number remains nearly constant and show some scattering. It is considered that this is due to the flow transition from laminar to turbulent.

Experimental Results using FC-40

To investigate the characteristics of liquid film thickness at relatively high capillary number and small Reynolds number, FC-40 is adopted as working fluid. Figure 12 shows the Reynolds number against capillary number in each fluid. Reynolds number of FC-40 is about 6 times smaller than that of ethanol at same capillary number.

Figure 13 shows the results using FC-40. Dimensionless liquid film thicknesses of five tubes at small capillary number become nearly identical also for FC-40. As capillary number increases, the trend of liquid film thickness becomes different from the cases of ethanol and water. All data become smaller than the Taylor's law. Liquid film thickness of 1.3 mm inner diameter tube is lower than that of 0.3 mm inner diameter tube although the Reynolds number of 1.3 mm tube is larger than that of 0.3 mm tube. Reynolds numbers of 1.3 mm and 0.3 mm inner diameter tubes are $Re = 151$ and 34 at $Ca = 0.05$. It means that the inertia force makes liquid film thinner at small Reynolds numbers. As capillary number increases, liquid film thickness of $D = 1.3$ mm tube becomes larger than that of $D = 0.3$ mm tube like the trend of water and ethanol.

Figure 14 shows the comparison with numerical simulation results obtained by Kreutzer et al. [8]. Present results are in good agreement with the numerical simulation results at cap-

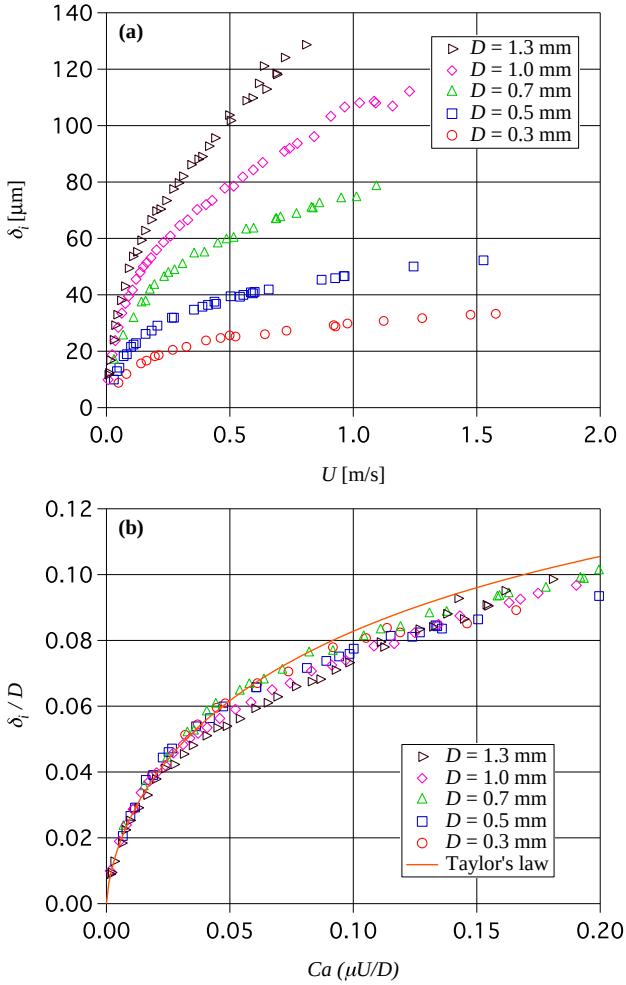

Figure 13. The results using FC-40: (a) Liquid film thickness against bubble velocity (b) Dimensionless liquid film thickness (δ_i/D) against capillary number ($Ca = \mu U/\sigma$)

illary number lower than 0.02. At high capillary number, it is confirmed that the liquid film thickness decreases at first and then increases as Reynolds number increases.

Scaling Analysis

Aussillous and Quere [6] showed additional scaling analysis to Bretherton's theoritical relation on the liquid film thickness. They replaced the curvature of bubble nose $\kappa = 1/R$ with $\kappa = 1/(R\text{-}\delta_i)$ and obtained the following relation:

$$\frac{\delta_i}{R} \sim \frac{Ca^{\frac{2}{3}}}{1+Ca^{\frac{2}{3}}}. \tag{2}$$

In Eq. (2), dimensionless liquid film thickness converges to a finite fraction of the tube diameter due to the term $Ca^{2/3}$ in the denominator. Based on Eq. (2), Taylor's experimental data was fitted as Eq. (1). However, the effect of inertia force on liquid film thickness is not taken into account in Eq. (2). If the effect of inertia force is taken into account, the momentum balance and the curvature matching between the bubble nose and the transition region should be expressed as follows:

$$\frac{\mu U}{\delta_i^2} \sim \frac{1}{\lambda}\left(\frac{\sigma}{R-\delta_i}\right) - \frac{1}{\lambda}\rho U^2, \tag{3}$$

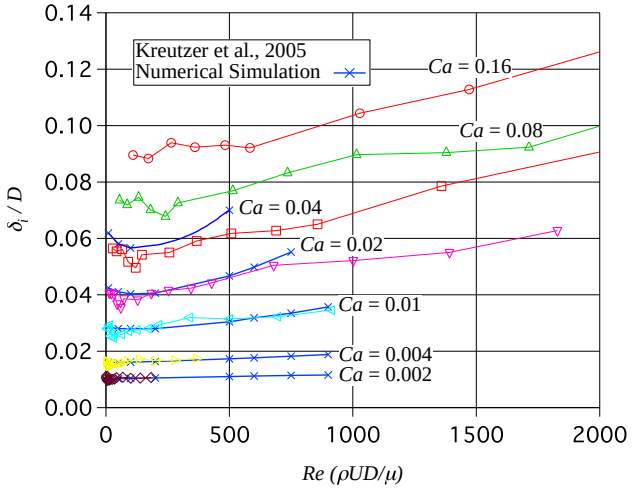

Figure 14. Dimensionless liquid film thickness (δ_i/D) against Reynolds number ($Re = \rho UD/\mu$)

$$\frac{\delta_i}{\lambda^2} \sim \frac{\sigma}{R-\delta_i}. \tag{4}$$

We can deduce the relation δ_i/R of from Eq. (3) and (4) as:

$$\frac{\delta_i}{R} \sim \frac{Ca^{\frac{2}{3}}}{Ca^{\frac{2}{3}}+(1-We')^{\frac{2}{3}}}, \tag{5}$$

where Weber number is defined as $We' = \rho U^2(R\text{-}\delta_i)/\sigma$. Equation (5) is always larger than Eq. (2) because the sign in front of Weber number is negative. Therefore, Eq. (5) can explain why liquid film thickness increases against Reynolds number. However, inertia force does not always make the liquid film thicker. Inertia force make liquid film thicker at high Reynolds number but the trend becomes opposite at small Reynolds number. This trend is confirmed by several numerical simulation results [7][8] and the present experimental results, as shown in Fig. 14. Heil [7] reported that at finite Reynolds number, inertia force make bubble nose more slender and decreases the radius of bubble nose curvature. This means that $\kappa = 1/(R\text{-}\delta_i)$ term in momentum equation should become larger with Reynolds number. We assume that this effect of inertia force can be expressed by adding a function of Reynolds number and capillary number to $\kappa = 1/(R\text{-}\delta_i)$ term as:

$$\kappa = \frac{1+f(Re,Ca)}{R-\delta_i}. \tag{6}$$

Substituting Eq. (6) in Eqs. (3) and (4), we obtain following relation:

$$\frac{\delta_i}{R} \sim \frac{Ca^{\frac{2}{3}}}{Ca^{\frac{2}{3}}+(1+f(Re,Ca))(1-\frac{We'}{1+f(Re,Ca)})^{\frac{2}{3}}}. \tag{7}$$

If we assume that the terms of Reynolds number, capillary number and Weber number are small, we may simplify Eq. (7) as:

$$\frac{\delta_i}{R} \sim \frac{Ca^{\frac{2}{3}}}{Ca^{\frac{2}{3}}+1+f(Re,Ca)-g(We')}. \tag{8}$$

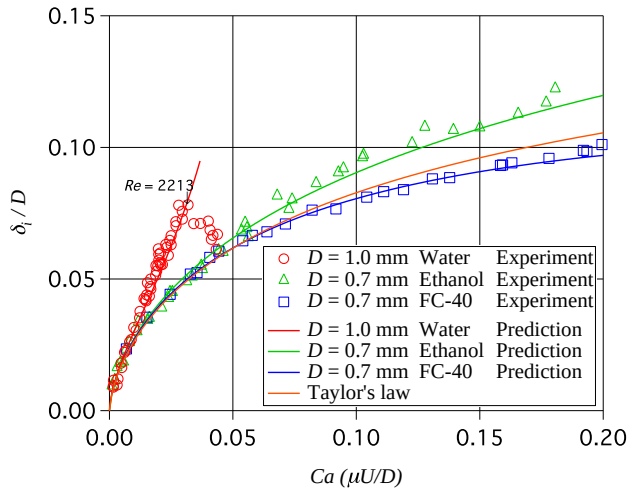

Figure 15. Predicted liquid film thickness (δ_i/D) against capillary number ($Ca = \mu U/\sigma$)

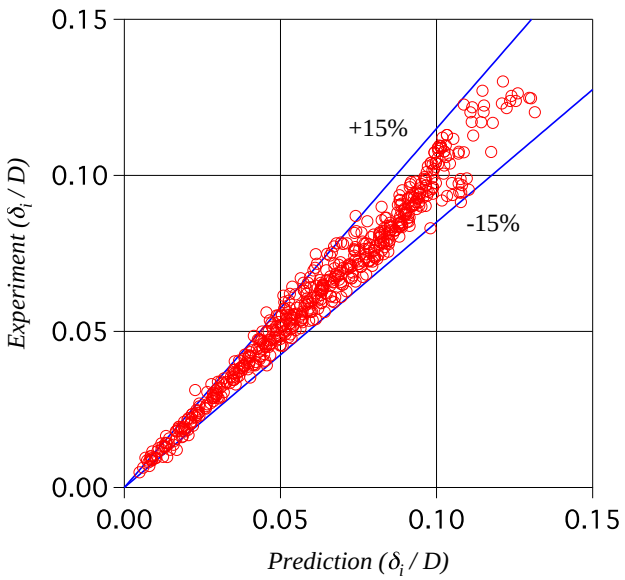

Figure 16. Comparison between the prediction values and the experimental results

In the denominator of Eq. (8), $f(Re,Ca)$ term correspond to the curvature change of bubble nose and contributes to reduce the liquid film thickness. On the contrary, when the inertia effect increases, $g(We')$ term contributes to increase the liquid film thickness due to the inertia effect in the momentum equation. Weber number in Eq. (5) has liquid film thickness δ_i in its definition, but it becomes complicated to use such a definition for the correlation. Therefore, Weber number defined as $We = \rho U^2 D/\sigma$ is used for the correlation. The experimental data is finally correlated in the form as:

$$\frac{\delta_i}{D} = \frac{0.67Ca^{\frac{2}{3}}}{1+3.13Ca^{\frac{2}{3}}+0.504Ca^{0.672}Re^{0.589}-0.352We^{0.629}}, \quad (9)$$

where $Ca = \mu U/\sigma$ and $Re = \rho UD/\mu$. As capillary number approaches zero, liquid film thickness should follow Bretherton's theory, so that the coefficient of numerator is taken as 0.67. Coefficients were obtained by least linear square fitting. In the present correlation, data of $Ca < 0.3$ and $Re < 2000$ were used. Figures 15 and 16 show the comparison between the prediction of Eq. (9) and the experimental data. As shown in Fig. 16 Eq. (9) can predict δ_i within $\pm 15\%$ error.

CONCLUSIONS

The liquid film thickness in micro tube is measured directly by laser focus displacement meter. Liquid film thickness changes according to the measuring position due to the effect of gravity. However, initial thickness δ_i is independent of the measuring position for $Bo{\cdot}Ca^{2/3} < 0.1$. Liquid slug length has nearly no effect on liquid film thickness in the present experiments. However, liquid film thickness becomes thicker when $L_{bubble} < 3D$. It is thought that liquid film thickness of short bubbles is affected by the bubble tail.

Liquid film thickness becomes thicker as velocity increases and tube diameter becomes larger. At small capillary number, liquid film thickness is determined only by capillary number and inertia effect is negligible. As capillary number increases, the effect of inertia force can not be neglected and liquid film thickness is determined by force balance between viscous, surface tension and inertia forces. At relatively large capillary number, liquid film thickness shows minimum against Reynolds number. If Reynolds number becomes larger than roughly 2000, liquid film thickness becomes nearly constant against capillary number and shows some scattering. Empirical correlation for the liquid film thickness based on capillary number, Reynolds number and Weber number is proposed. The correlation can predict the experimental results within $\pm 15\%$ error.

ACKNOWLEDGEMENT

We would like to thank Prof. Kasagi and Prof. Suzuki for the fruitful discussions and suggestions. This work is supported through Grant in Aid for Scientific Research (No. 20560179) by MEXT, Japan.

NOMENCLATURE

Bo Bond number
Ca Capillary number
D Tube diameter, [m]
g Acceleration of gravity, [m/s^2]
n Refractive index
We Weber number
Re Reynolds number
R Tube radius, [m]
U Bubble velocity, [m/s]

Greek Symbols
δ Liquid film thickness, [m]
κ Curvature of bubble nose, [m^{-1}]
λ Length of transition region, [m]
μ Viscosity, [Pa·s]
ρ Density, [kg/m^3]
σ Surface tension coefficient, [N/m]

Subscripts
bottom Tube bottom in horizontal flow direction
center Tube center in horizontal flow direction
i Initial

REFERENCES

[1] J. R. Thome, V. Dupont and A. M. Jacobi, Heat transfer model for evaporation in microchannels. Part : presentation of the model, *Int. J. Heat Mass Transfer*, Vol. 47, pp. 3375 - 3385, 2004.

[2] D. B. R. Kenning, D. S. Wen, K. S. Das and S. K. Wilson, Confined growth of a vapour bubble in a capillary tube at initially uniform superheat: Experiments and modeling, *Int. J. Heat Mass Transfer*,Vol. 49, pp. 4653 - 4671, 2006.

[3] G. I. Taylor, Deposition of a viscous fluid on the wall of a tube, *J. Fluid Mech.*, Vol. 10, pp. 1161-1165, 1961.

[4] F. P. Bretherton, The motion of long bubbles in tubes, *J. Fluid Mech.*, Vol. 10, pp. 166 - 188, 1961.

[5] K. Moriyama and A. Inoue, Thickness of the liquid film formed by a growing bubble in a narrow gap between two horizontal plates, *Trans. of the ASME*, Vol. 118, pp. 132 - 139, 1996.

[6] P. Aussillous and D. Quere, Quick deposition of a fluid on the wall of a tube, *Phys. of Fluids*, Vol. 12, pp. 2367 - 2371, 2000.

[7] M. Heil, Finite Reynolds number effects in the Bretherton problem, *Phys. of Fluids*, Vol. 13, pp. 2517 - 2521, 2001

[8] M. T. Kreutzer, F. Kapteijn, J. A. Moulijn, C. R. Kleijn and J. J. Heiszwolf, Inertial and interfacial effects on pressure drop of Taylor flow in capillaries, *AIChE J.*, Vol. 51, pp. 2428 - 2440, 2005.

[9] Y. Utaka, S. Okuda and Y. Tasaki, Structure of micro-layer and characteristics of boiling heat transfer in narrow gap mini-channel system, *Trans. of the JSME, Series B*, Vol. 73, pp. 1929 - 1935, 2007.

[10] T. Takamasa and K. Kobayashi, Measuring interfacial waves on film flowing down tube inner wall using laser focus displacement meter, *J. Multiphase Flow*, Vol. 26, pp. 1493 - 1507, 2000.

[11] T. Hazuku, N. Fukamachi, T. Takamasa, T. Hibiki and M. Ishii, Measurement of liquid film in microchannels using a laser focus displacement meter, *Experiments in Fluids*, Vol. 38, pp.780 - 788, 2005.